Control Of Buck and Boost Converters For Stand-Alone DC Microgrids

Daniel Zammit[1*], Cyril Spiteri Staines[1], Maurice Apap[1], Alexander Micallef[1]

[1]*Department of Industrial Electrical Power Conversion, Faculty of Engineering, University of Malta, Msida, MSD 2080, Malta*

**daniel.zammit@um.edu.mt*

Abstract - **This paper presents the modelling and control of Buck and Boost converters to be operated in a stand-alone DC Microgrid. The Buck and Boost converters can be considered as the basis of a number of other converters, therefore the control system presented can be extended to other similar applications. The two converters can be used to interface photovoltaic (PV) panels or wind turbine systems to a DC microgrid. In this paper both converters will be modelled in continuous conduction mode (CCM), and the control system needed to operate these converters in a stand-alone DC microgrid will be presented. The inductor current and the output voltage of the converter will be controlled using nested control loops. The droop control method will be utilized to obtain load sharing between the converters when these are paralleled in the microgrid. An outer addition voltage restoration loop will be applied to restore the desired voltage in the dc microgrid, correcting any voltage deviations caused by the droop control method. The operation of the control loops will be tested by simulations. The simulation model will consist of two paralleled Buck converters operated in CCM, while sharing a common resistive load.**

Keywords - **DC Microgrid, Buck, Boost, Converter, Control, Droop, Proportional-Integral.**

I. INTRODUCTION

Distributed power generation systems can be combined with energy storage systems as well as consumer loads to form a microgrid. A microgrid can be AC, DC or a combination of both, depending on its particular utilisation and application. The concept of the microgrid has gained popularity due to the increasing number of distributed power generation systems, as well as its ability to form a self sustainable electrical grid system. In fact a very attractive aspect of the microgrid is the ability to operate both in grid-connected mode as well as in islanded mode. In grid-connected mode the microgrid is connected through a coupling point to the electrical grid, while in islanded or stand-alone mode the microgrid is operated in an autonomous way disconnected from the electrical grid. The islanded mode provides the advantage of isolated operation in case of an electrical grid failure. The stand-alone mode of operation can provide electrical supply in remote, isolated and rural areas, where the provision of a national AC grid is difficult or highly unlikely to be achieved.

Different scenarios call for different AC or DC microgrid configurations, but DC microgrids are highly being researched due to the number of advantages offered. A DC microgrid offers a number of advantages like; lower conversion losses due to less conversion stages (dc to ac and vis-versa), no synchronisation, phase or frequency issues, and independence from voltage sags, dips, and other power quality issues occurring on the electrical AC grid side. These advantages make the DC microgrid attractive for use with consumer electronics (where generally the main circuitry is DC operated), electric vehicle charging, telecommunication equipment, as well as military equipment. Fig. 1 shows an example of a DC microgrid.

Research is being carried out to optimize and facilitate the connection of renewable energy sources like photovoltaic systems and wind turbine systems, as well as energy storage systems like batteries and super-capacitors with various loads [1]. Current research on DC microgrids covers various aspects like modelling, control design and stability testing of the various converters and systems integrated in the DC microgrid. Other aspects being researched are electrical energy storage and energy management within the DC microgrid [1-10]. The selection of the converters and control systems used is very important for proper operation of the DC microgrid. Various literature cover different aspects of converter and DC microgrid control. In [2] a hierarchical control system for microgrids was proposed consisting of three levels. The first level or primary control is based on the droop method for common load sharing. The second level or secondary control restores deviations caused by the primary control while the third level or tertiary control manages the power flow between the microgrid and external electrical distribution systems. In [1] and [3] the control system is extended to multiple DC microgrids connected together, to regulate power flow among the microgrids as well as the overall stability of the connected systems.

This paper presents the modelling of the Buck and Boost converters which can be considered as an option for interfacing photovoltaic (PV) panels and wind turbine systems with a DC microgrid infrastructure. These particular two converter topologies were selected since they can be considered as the basis for other converters. The Buck and Boost converters operated in continuous conduction mode (CCM) will be modelled, and the control system for these

converters to operate in stand-alone mode will be presented and discussed.

The paper is organized as follows. Sections 2 and 3 describes the converter and control modelling, respectively. Section 4 covers the DC microgrid simulation, while the simulation results are presented in Section 5. Section 6 contains the conclusion with the final remarks.

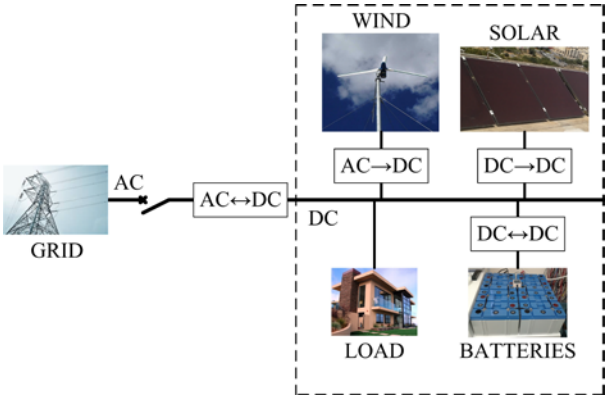

Fig. 1, DC Microgrid.

II. Converter Modelling

2.1. Buck Converter

The Buck Converter shown in Fig. 2 is a switching converter that produces a lower average output voltage (V_o) than the dc input voltage (V_{in}).

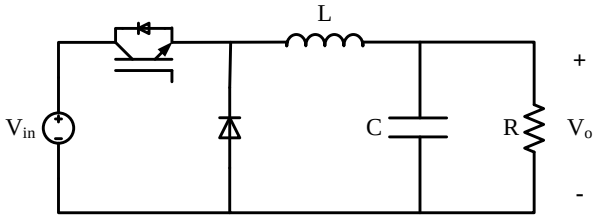

Fig. 2, Buck Converter.

For the Buck converter, the voltage conversion ratio of the output voltage to the input voltage ($M(D)$), which is a function of the Duty Cycle (D) is given by:

$$M(D) = \frac{V_o}{V_{in}} = D \tag{1}$$

The Buck converter inductor (L) value can be found by:

$$L = \frac{(V_{in} - V_o)D}{2\Delta i_L f_s} \tag{2}$$

where, Δi_L is the desired inductor current peak ripple, and f_s is the switching frequency of the Buck converter.

The Buck converter capacitor (C) value can be found by:

$$C = \frac{\Delta i_L}{8\Delta v_o f_s} \tag{3}$$

where, Δv_o is the desired output voltage peak ripple.

2.2. Buck Converter Model

The CCM small signal equivalent model of the Buck converter shown in Fig. 3 is derived using the linearized small signal mathematical equations given by Equations (4), (5) and (6).

$$L\frac{d\hat{i}_L(t)}{dt} = D\hat{v}_{in} + \hat{d}V_{in} - \hat{v}_o(t) \tag{4}$$

$$\hat{i}_c(t) = C\frac{d\hat{v}_o(t)}{dt} = \hat{i}_L(t) - \frac{\hat{v}_o(t)}{R} \tag{5}$$

$$\hat{i}_{in}(t) = D\hat{i}_L(t) + \hat{d}I_L \tag{6}$$

where, $\hat{i}_L(t)$, $\hat{i}_c(t)$, $\hat{i}_{in}(t)$, $\hat{d}$, $\hat{v}_{in}(t)$, and $\hat{v}_o(t)$ are small ac variations around the quiescent values for the inductor current, capacitor current, input current, duty cycle, input voltage, and output voltage, respectively. I_L is the average inductor current, and R is the load resistance.

The equivalent circuit in Fig. 3 can by simplified to obtain the version shown in Fig. 4, which is more intuitive to obtain the required transfer functions.

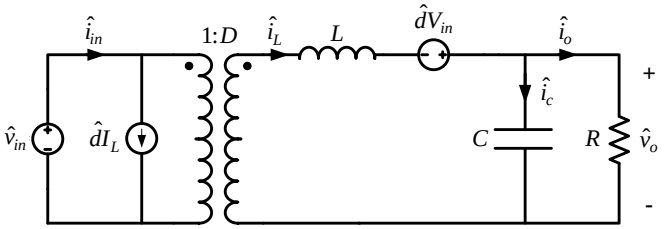

Fig. 3, Buck Converter Small Signal Equivalent Circuit.

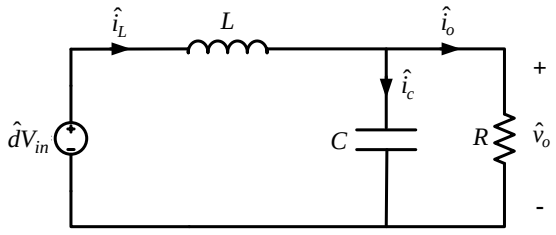

Fig. 4, Buck Converter Simplified Small Signal Equivalent Circuit.

By transforming the small signal mathematical model equations to the s-domain and using the small signal equivalent circuit the transfer functions of the duty cycle to the inductor current $G_{id}(s)$ and the inductor current to the output voltage $G_{vi}(s)$ can be obtained:

$$G_{id}(s) = \frac{\hat{i}_L(s)}{\hat{d}} = \frac{V_{in}(sCR+1)}{s^2CLR + sL + R} \tag{7}$$

$$G_{vi}(s) = \frac{\hat{v}_o(s)}{\hat{i}_L(s)} = \frac{R}{sCR+1} \tag{8}$$

2.3. BOOST CONVERTER

The Boost Converter shown in Fig. 5 is a switching converter that produces a higher average output voltage (V_o) than the dc input voltage (V_{in}).

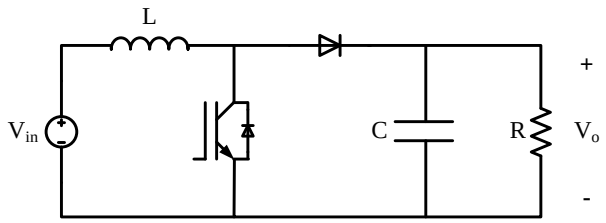

Fig. 5, Boost Converter.

For the Boost converter, the voltage conversion ratio of the output voltage to the input voltage ($M(D)$), which is a function of the Duty Cycle (D) is given by:

$$M(D) = \frac{V_o}{V_{in}} = \frac{1}{1-D} \tag{9}$$

The Boost converter inductor (L) value can be found by:

$$L = \frac{V_{in} D}{2\Delta i_L f_s} \tag{10}$$

where, Δi_L is the desired inductor current peak ripple, and f_s is the switching frequency of the Boost converter.

The Boost converter capacitor (C) value can be found by:

$$C = \frac{V_o D}{2\Delta v_o R f_s} \tag{11}$$

where, Δv_o is the desired output voltage peak ripple, and R is the load resistance.

2.4. BOOST CONVERTER MODEL

The CCM small signal equivalent model of the Boost converter shown in Fig. 6 is derived using the linearized small signal mathematical equations given by Equations (12), (13) and (14).

$$L\frac{d\hat{i}_L(t)}{dt} = \hat{v}_{in}(t) - D'\hat{v}_o(t) + \hat{d}V_o \tag{12}$$

$$\hat{i}_c(t) = C\frac{d\hat{v}_o(t)}{dt} = -\frac{\hat{v}_o(t)}{R} + D'\hat{i}_L(t) - \hat{d}I_L \tag{13}$$

$$\hat{i}_{in}(t) = \hat{i}_L(t) \tag{14}$$

where, $\hat{i}_L(t)$, $\hat{i}_c(t)$, $\hat{i}_{in}(t)$, $\hat{d}$, $\hat{v}_{in}(t)$, and $\hat{v}_o(t)$ are small ac variations around the quiescent values for the inductor current, capacitor current, input current, duty cycle, input voltage, and output voltage, respectively. I_L is the average inductor current, and R is the load resistance.

The equivalent circuit in Fig. 6 can by simplified to obtain the version shown in Fig. 7, which is more intuitive to obtain the required transfer functions.

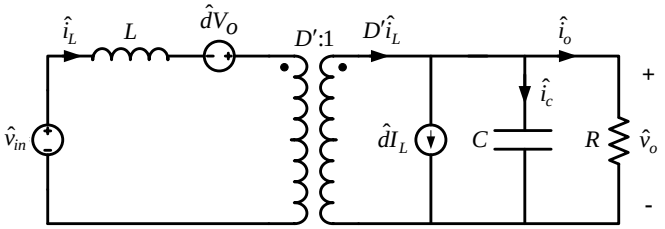

Fig. 6, Boost Converter Small Signal Equivalent Circuit.

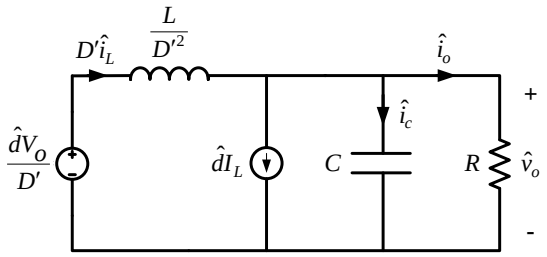

Fig. 7, Boost Converter Simplified Small Signal Equivalent Circuit.

By transforming the small signal mathematical model equations to the s-domain and using the small signal equivalent circuit the transfer functions of the duty cycle to the inductor current $G_{id}(s)$ and the inductor current to the output voltage $G_{vi}(s)$ can be obtained:

$$G_{id}(s) = \frac{\hat{i}_L(s)}{\hat{d}} = \frac{sCRV_o + V_o + I_L RD'}{s^2 CLR + sL + RD'^2} \tag{15}$$

$$G_{vi}(s) = \frac{\hat{v}_o(s)}{\hat{i}_L(s)} = \frac{D'V_o R - sLRI_L}{sCRV_o + V_o + I_L RD'} \tag{16}$$

III. CONTROL SYSTEM MODELLING

When the DC microgrid is in stand-alone or islanded mode the control system consists of two nested Proportional Integral (PI) control loops. The inner loop controls the inductor current and outer loop controls the output voltage of the converter. The inner current control loop should be faster than the outer voltage control loop to minimize interaction between the two loops and therefore prevent instability. The droop control method is utilized to obtain load sharing between paralleled converters within the DC microgrid, preventing any circulating currents between the converters. The control also includes another outer loop utilizing a PI controller to restore the voltage in the DC microgrid to the desired level, by correcting any voltage deviations caused by the droop control method. This outer control loop is referred to as the voltage restoration control loop, and is common to all the converters within the DC microgrid. Fig. 8 shows the block diagram of the control system including the droop control loop.

The current and voltage PI controllers, $C_i(s)$ and $C_v(s)$, respectively, are of the form:

$$C(s) = K_p + \frac{K_I}{s} \tag{17}$$

where, K_P is the Proportional Gain term, and K_I is the Integral term.

The plant transfer function $P_i(s)$ for the current PI controller is obtained by:

$$P_i(s) = T_{mod} \times G_{id}(s) \tag{18}$$

where, T_{mod} is the transfer function representing the pulse width modulation stage.

The pulse width modulation stage produces the duty cycle d that is proportional to the control voltage v_c. The pulse width modulator makes a comparison between the control voltage v_c and a sawtooth waveform with a peak to peak amplitude V_m. The value for V_m is selected by the designer. The frequency of the sawtooth waveform corresponds to the desired converter switching frequency f_s. This comparison is used to determine the switching on/off of the converter switch. The pulse width modulation stage can be modelled by the transfer function T_{mod} given by:

$$T_{mod} = \frac{1}{V_m} \tag{19}$$

The plant transfer function $P_v(s)$ for the voltage PI controller is obtained by:

$$P_v(s) = \frac{C_i(s)P_i(s)}{1 + C_i(s)P_i(s)} \times G_{vi}(s) \tag{20}$$

To connect two or more converters in parallel sharing a common load the droop control method is used. This prevents any circulating current between the converters in case there are any differences in the output voltages. The droop method prevents circulating currents between converters by adjusting the voltage reference provided to the voltage and current control loops. This control method is applied by inserting an additional loop with a virtual resistance R_{droop} as shown in Fig. 8. The output voltage v_o can be expressed as:

$$v_o = V_{ref} - R_{droop} i_L \tag{21}$$

where, V_{ref} is the output voltage reference at no load, and i_L is the inductor current (or output current i_o, depending on the current sensed and utilised in the control loop).

The value for the virtual resistance can be calculated using:

$$R_{droop} = \frac{\varepsilon_v}{i_{o\_max}} \tag{22}$$

where, ε_v is the maximum permissible voltage deviation, and i_{o_max} is the maximum output current.

The droop control loop permits sharing of a common load between paralleled converters but causes a load dependent output voltage deviation. The voltage deviation problem can be solved by the application of another controller which restores the microgrid voltage to the desired level. This controller will form another outer control loop common to all the converters/sources in the microgrid. In this control loop the microgrid voltage will be compared with the desired voltage, and the PI compensator of the loop will generate the needed value for correct voltage restoration required by the converter control systems in the microgrid. Fig. 9 shows the block diagram of the voltage restoration control loop which is connected to all the converters making up the DC microgrid.

The voltage restoration PI controller C_{res} is of the form shown in Equation (17). The demanded value of the voltage restoration loop V_{mgref} is set to the desired DC microgrid voltage. The actual DC bus microgrid voltage V_{mg} is measured and fed back to this loop for the controller to generate the required restoration voltage V_{res}, as shown in Fig. 9. The value of V_{res} should be restricted within limits to prevent it from exceeding the maximum allowed voltage deviation.

The output voltage v_o equation is modified to include this restoration voltage as follows:

$$v_o = V_{ref} + V_{res} - R_{droop} i_L \tag{23}$$

The plant transfer function $P_{res}(s)$ for the voltage restoration PI controller is obtained by:

$$P_{res}(s) = \frac{C_v(s)P_v(s)}{1 + C_v(s)P_v(s)(1 + \frac{R_{droop}}{G_{vi}(s)})} \tag{24}$$

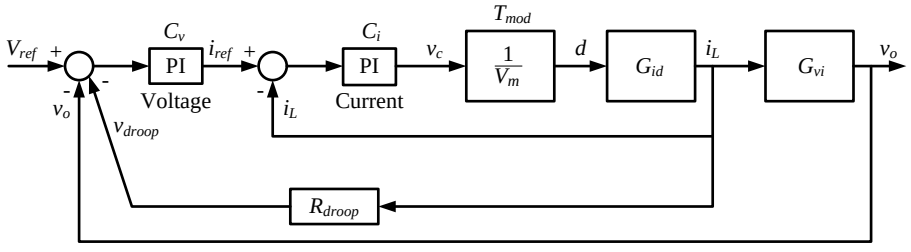

Fig. 8, Block Diagram of the Control System with Current and Voltage Control including the Droop Loop.

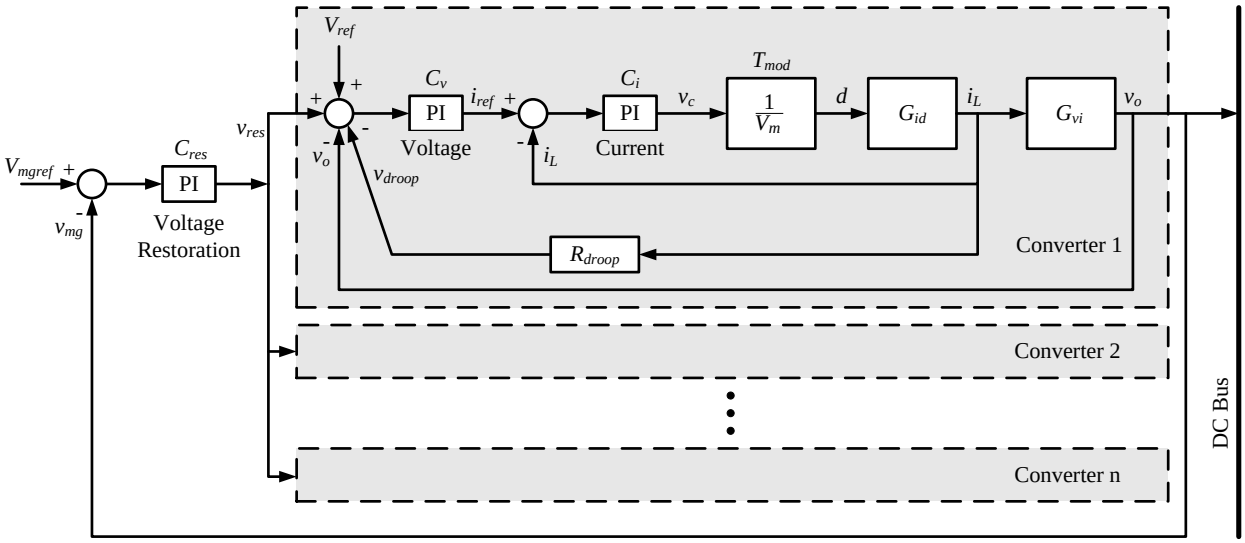

Fig. 9, Block Diagram of the Voltage Restoration Control Loop.

IV. DC Microgrid Simulation

Two 2.5kW buck converters with their control system were modelled and simulated using Matlab/Simulink. The parameters and values for the buck converters and the controllers are listed in Tables 1 and 2, respectively. The design of the buck converter was carried out using Equations (1), (2) and (3) to calculate the duty cycle *D*, the inductor *L* and the capacitor *C*, respectively. The predefined set parameters and the calculated values are shown in Table 1. The inductor resistance R_L and the equivalent series resistance (ESR) of the capacitor R_c were taken from actual inductor and capacitor data. The droop resistance was calculated using Equation (22). The maximum percentage voltage deviation was taken to be 10% of the output voltage, thus obtaining a droop resistance of 0.09216Ω. Transfer functions (18), (20) and (24) were used to design the current, voltage, and voltage restoration PI controllers, respectively, using Matlab. The value for V_m was selected to be 100V, a voltage value which is equal to the expected dc voltage of the energy source. The load resistance *R* value was taken as 0.9216 Ω for the PI controllers design, which is the value of load resistance needed for the converter to operate at maximum load current. The values for the proportional gain term K_P and the integral term K_I for each PI controller are listed in Table 2. The bandwidths for the current, voltage, and voltage restoration closed loops obtained are 134Hz, 0.65Hz and 0.01Hz, respectively. The droop loop of each converter permitted sharing of the load when the converters were parallel connected, and the voltage restoration controller was used to restore the microgrid bus voltage to the required 48V. Fig. 10 shows the two paralleled buck converters and the voltage restoration control system. Fig. 11 and Fig. 12 show the control system of the buck converter and buck converter power stage modelled in Simulink, respectively.

A simulation was performed with two paralleled buck converters to test the operation of a 48V DC microgrid, including load sharing between the converters. Initially only one converter was switched on, and supplied a resistive load of 0.9216 Ω. After 3sec another converter was connected in parallel with the first converter, thus sharing the resistive load. When the two buck converters were connected in parallel the droop loop of each converter adjusted the output voltage of each converter to obtain load current sharing. After 25sec the voltage restoration control loop was switched on, which started to restore the DC microgrid voltage back to 48V.

TABLE 1, Buck Converter Parameters

Set Parameters	
Input Voltage V_{in}	100V
Output Voltage V_o	48V
Switching Frequency f_s	10kHz
Converter Power *P*	2.5kW
Inductor current peak to peak percentage ripple	10%
Output voltage peak percentage ripple Δv_o	0.5%
Inductor Resistance R_L	0.002Ω
ESR of Capacitor R_c	0.03Ω
Calculated Values	
Duty Cycle *D*	0.48
Inductor *L*	0.479mH
Capacitor *C*	271.25μF

TABLE 2, PI Controllers Values

Current PI K_P	1.144
Current PI K_I	880
Voltage PI K_P	0.0644
Voltage PI K_I	4.6
Voltage Restoration PI K_P	0.00102
Voltage Restoration PI K_I	0.06

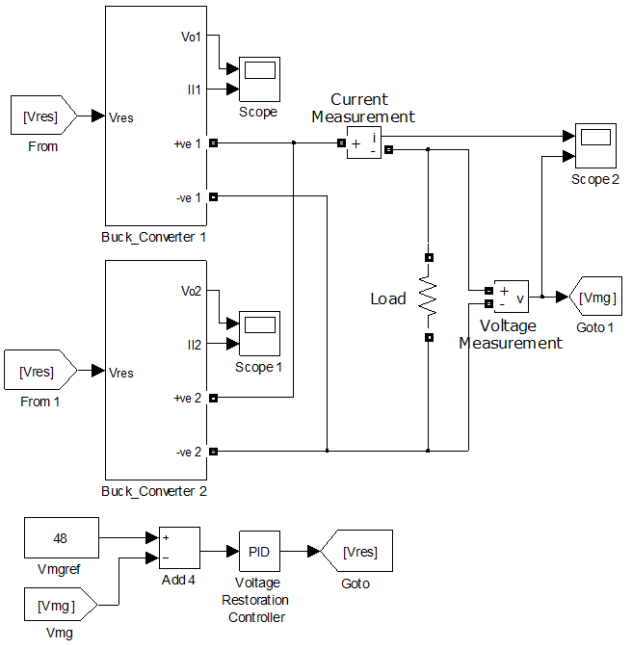

Fig. 10, Paralleled Buck Converters and the Voltage Restoration Control Loop.

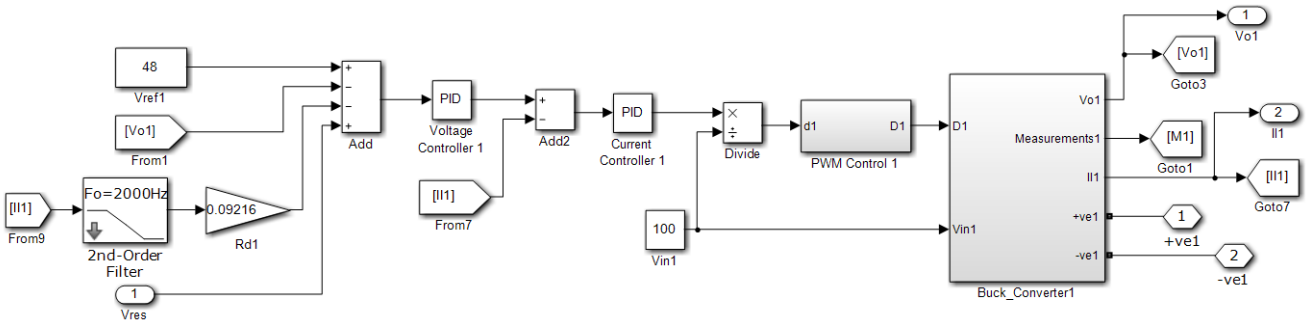

Fig. 11, Cascaded Current and Voltage Control System.

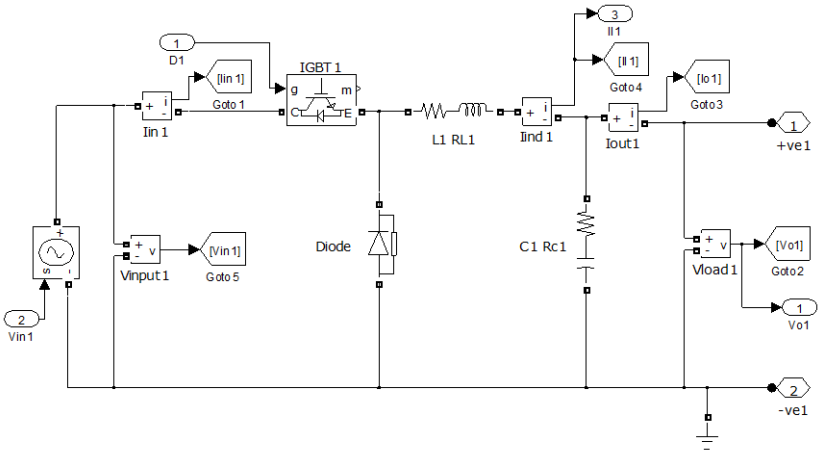

Fig. 12, Buck Converter Modelled in Simulink.

V. Simulation Results

The simulation results are shown in Fig. 13 up to 16. Fig. 13 shows the output currents for the two buck converters (I_{o1} and I_{o2}) and the total output current through the resistive load (I_o). Fig. 14 shows the output voltage (V_o). Both Figs. 13 and 14 show the start-up of the first converter at a time of 0sec, the instant when the second converter was connected at a time of 3sec, and also the switching ON of the voltage restoration control loop at a time of 25sec. The results show the successful operation of the current and voltage control loops, as well as the load sharing due to the droop control loops. The voltage restoration control loop corrected the output voltage variation caused by the droop control back to 48V after about 120secs, as shown in Figs. 15 and 16. Fig. 15 show the output currents for the two buck converters and the total output current when the DC microgrid voltage was restored to 48V. Fig. 16 shows the output voltage being restored at 48V at 120secs.

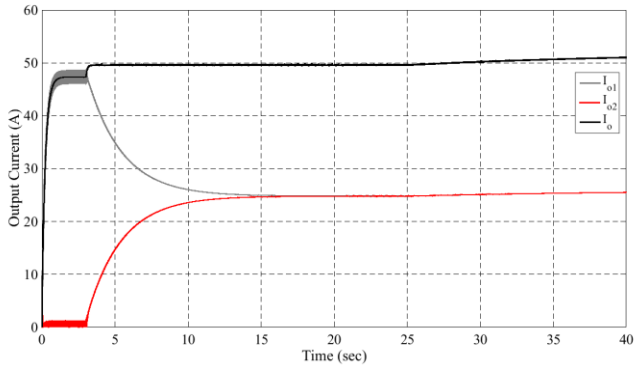

Fig. 13, Output Currents.

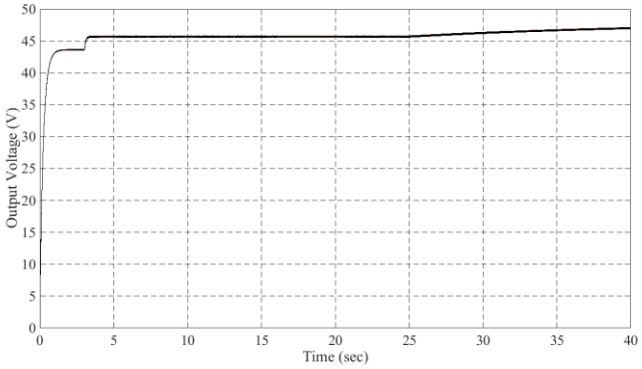

Fig. 14, Output Voltage.

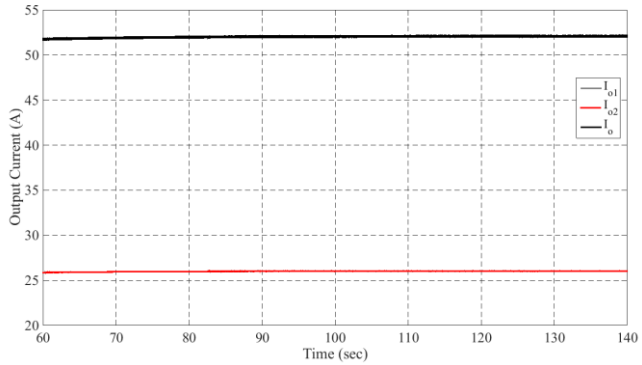

Fig. 15, Output Currents with 48V.

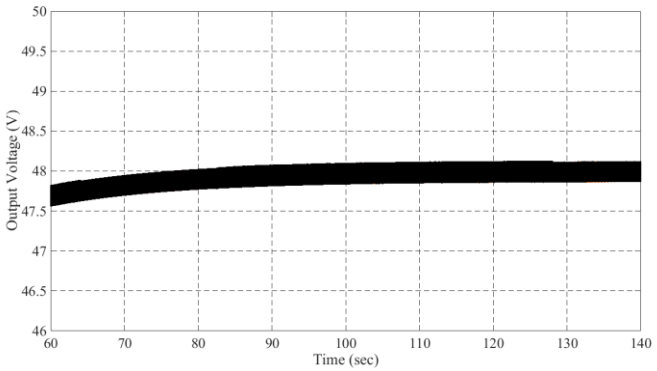

Fig. 16, Output Voltage at 48V.

VI. Conclusion

This paper presented an overview on the buck and boost converters, including the control system to operate in a DC microgrid. Modelling of the buck and boost converters in CCM was presented, and the small signal equivalent circuit was derived. The small signal equivalent circuit was used to obtain the transfer functions needed for the design of the current and voltage controllers of the converters. The droop control method was applied by an additional loop in the control system to permit sharing of a common load by multiple paralleled converters in the DC microgrid. The droop control method causes small output voltage variation from the set DC microgrid voltage. This voltage variation was catered for by the use of the voltage restoration loop. This additional outer loop restores the output voltage of all the converters in the microgrid to the preset voltage value of the DC microgrid. The discussed converter design, modelling, and control procedures were tested by simulating two buck converters connected in parallel sharing a common resistive load.

References

[1] Q. Shafiee, T. Dragicevic, J. C. Vasquez and J. M. Guerrero, “Modeling, Stability Analysis and Active Stabilization of Multiple DC-Microgrid Clusters”, Energycon 2014, Dubrovnik, Croatia, May 2014.

[2] J. M. Guerrero, J. C. Vasquez, J. Matas, L. G. de Vicuna and M. Castilla, “Hierarchical Control of Droop-Controlled AC and DC Microgrids – A General Approach Towards Standardization”, IEEE Transactions on Industrial Electronics, Vol. 58, No. 1, January 2011.

[3] Q. Shafiee, T. Dragicevic, J. C. Vasquez and J. M. Guerrero, “Heirarchical Control for Multiple DC-Microgrids Clusters”, IEEE Transactions on Energy Conversion, Vol. 29, No. 4, December 2014.

[4] S. Anand and B. G. Fernandes, “Optimal Voltage Level for DC Microgrids”, 36th Annual Conference (IECON 2010), IEEE Industrial Electronics Society, November 2010.

[5] P. Karlsson and J. Svensson, “Voltage Control and Load Sharing in DC Distributed Systems”, European Power

Electronics Conference (EPE 2003), Toulouse, France, September 2003.

[6] B. M. Han and H. J. Kim, "Operation Analysis of Coordinated Droop Control for Stand-Alone DC Microgrid", International Conference on Renewable Energies and Power Quality (ICREPQ'14), Cordoba, Spain, April 2014.

[7] X. Lu, K. Sun, J. M. Guerrero, J. C. Vasquez and L. Huang, "State-of-Charge Balance Using Adaptive Droop Control for Distributed Energy Storage Systems in DC Microgrid Applications", IEEE Transactions on Industrial Electronics, Vol. 61, No. 6, June 2014.

[8] S. Anand and B. G. Fernandes, "Modified Droop Controller for Paralleling of DC-DC Converters in Standalone DC System", IET Power Electronics, Vol. 5, Issue 6, February 2012.

[9] Y. H. Huang, C. K. Tse and H. H. C. Lu, "Comparison of Configurations for Parallel DC/DC Converters", Australasian Universities Power Engineering Conference (AUPEC 2007), December 2007.

[10] R. Zamora and A. K. Srivastava, "Energy Management and Control Algorithms for Integration of Energy Storage Within Microgrid", 23rd International Symposium on Industrial Electronics (ISIE 2014), June 2014.